ELSEVIER

0309-1708(95)00001-1

Advances in Water Resources, Vol. 18, No. 2, 89–100, 1995

0309-1708/95/$09.50+0.00

Critical assessment of the operator-splitting technique in solving the advection–dispersion–reaction equation: 1. First-order reaction

Jagath J. Kaluarachchi & Jahangir Morshed

College of Engineering, Utah Water Research Laboratory, Utah State University, Logan, Utah 84322-8200, USA

(Received 18 February 1994; accepted 3 January 1995)

Operator-splitting technique (OST) is a common mathematical approach used in the solution of the advection–dispersion–reaction equation (ADRE), especially in the presence of biological decay, where the scales of transport and biological decay are far apart. The OST introduces a time-lag between the advection–dispersion and reaction stages by splitting the ADRE causing a breakdown of the physics of the problem, thus limiting its applicability. In this work, the applicability of the operator splitting technique is studied in parts. This first manuscript addresses the critical limitations of the operator-splitting technique as related to first-order decay, and the second manuscript extends the work to include coupled transport between hydrocarbon and oxygen with Monod kinetics describing biological decay. The critical assessment is performed to address the errors associated with the time-lag due to splitting. The assessment is based on mass balance errors, deviations of concentration prediction and sensitivities of concentration deviations. The results show that the splitting introduces an inherent error independent of the discretization errors. This inherent error increases with reaction rate and time-lag, and the overall errors can be reduced by using the alternate operator-splitting technique suggested by previous researchers.

INTRODUCTION

Biodegradation is considered to be a safe and economical method for remediating contaminated groundwater. A typical biodegradation process involves several coupled species such as the microbes, oxygen and hydrocarbon. Thus, modeling of biodegradation is mathematically complex. It usually involves Monod kinetics and generates a system of coupled nonlinear partial differential equations (PDE) to describe mass transport and degradation[1,2,6] whose time scales are often far apart. Solving such a system of equations requires small time steps and iterative procedures making the solution both time-consuming and expensive. To overcome these difficulties, many researchers have found the operator-splitting technique (OST) to be promising as it permits the use of schemes particularly suited to each part of the problem. In fact, many recent theoretical models have adopted the OST[3,4,7,11,16–18] to solve biodegradation problems. In solving such a problem, OST usually splits the nonlinear system of advection–dispersion–reaction equations (ADREs) into a system of linear partial differential equations involving the advection–dispersion equations (ADEs) and a system of nonlinear ordinary differential equations (ODEs) involving the reaction equations (REs). Assuming that the error caused by splitting is negligible, the accuracy of the OST in solving the ADRE depends on two independent criteria: (i) its ability to solve the ADE accurately, and (ii) its ability to solve the RE accurately. Although progress has been made in solving the ADE, it still remains an active area of research. In contrast, the RE is usually easy to solve using an ordinary differential equation integrator.

Valocchi and Malmstead[13] noted three attractive features of the OST for solving the ADRE. First, the OST allows the solution of each stage using a numerical scheme most suitable for that stage. The ADE is solved using a scheme usually based on finite difference or finite element methods while the RE is solved using an ordinary differential equation integrator based on finite difference or Runge-Kutta methods.[5] This feature also allows one to take advantage of the different time scales of each stage. As the time scale of the ADE is often much larger than that of the RE, the ADE can be solved using a time step (Δt) much larger than the time step, Δt_s, required by the RE (i.e. $\Delta t \gg \Delta t_s$). Chiang *et*

al.[4] solved the ADE using a finite element method coupled with the modified method of characteristics, and the RE using a second-order explicit Runge-Kutta method. Second, the OST can be implemented efficiently on parallel computers[17] where the ADE can be solved on different processors while the RE can be solved in parallel over as many processors as available. Third, the OST allows the development of a flexible modular code which can be easily extended or modified to handle alternative reaction submodels for the RE.

Wheeler and Dawson[17] gave a formal proof for the convergence of the OST for solving the ADRE. Strang[12] and LeVeque and Oliger[8] showed that time-splitting can introduce numerical errors for certain classes of operators; their observations were based on the OST work on hyperbolic problems in the numerical analysis literature. Valocchi and Malmstead[13] showed that time-splitting of the advection–dispersion operator from the reaction operator introduces an inherent error in the solution of the ADRE. They presented a critical assessment of the accuracy of the OST in the groundwater modeling literature. Before this assessment, the only published guideline on numerical accuracy suggested that each stage of the OST should be solved with small discretization errors to achieve an accurate overall solution. They showed the presence of an inherent mass balance error (MBE) in the OST algorithm for problems involving continuous mass flux boundary conditions. Such an MBE does not exist for instantaneous mass input problems. These conclusions were based on the MBE analysis of a simple one-dimensional first-order problem for which each stage of the calculation could be performed analytically (i.e. without discretization error). Finally they proposed an improved OST algorithm for the solution of the ADRE. This improved scheme was called the alternate operator-splitting technique (AOST). It was noted that AOST is closely related to the Strang splitting technique (SST) described by Strang[12] and LeVeque and Oliver.[8] In fact, the algorithm of SST and AOST are identical but the SST uses half the time steps of AOST.[9] As such, the SST is superior to AOST.[14] Also, it was noted that the half time steps of SST corresponded to odd time steps of AOST, while the full time steps of SST corresponded to even time steps of AOST. Finally, as Strang[12] and LeVeque and Oliger[8] have formally demonstrated that the SST has a higher order of accuracy in time than the normal operator-splitting technique (NOST), it appeared reasonable to accept AOST as a superior technique compared to NOST.

It is seen from the above review that the OST does have a potential for solving ADRE over a wide range of reaction terms. In order to implement the technique effectively, its behavior needs to be understood. Although Valocchi and Malmstead[13] did provide some light on the subject, their study was limited to a simple problem. The conclusions were drawn based on the mass balance error only, and little attention was paid to the concentration profile. The present study is an extension of this previous work to understand the overall applicability and limitations of the OST under different scenarios.

The work in this two-part series manuscript describes the applicability of the OST under a variety of reaction terms. These include first-order decay, Monod kinetics and coupled transport with biological decay. The applicability of the OST is assessed by considering the mass balance error, deviation of the concentration predictions and sensitivity of the concentration deviation to different parameters. Also two different approaches of the OST, namely the normal operator-splitting technique, NOST, and the alternate operator-splitting technique, AOST, are addressed. The first manuscript focuses on the simple first-order decay, and the second one addresses coupled transport with Monod kinetics.

THEORETICAL ANALYSIS

In a typical time step, the NOST solves the ADRE in two stages. In the first stage, the NOST solves the ADE, and in the second stage, it solves the RE using the solution of the first stage as the initial condition. In contrast, the AOST solves the ADRE over two time steps. In the first time step of a typical two time step interval, the technique is similar to the NOST. However, in the second time step, the order of solving ADE and RE are reversed.

At this stage, several key features of the NOST and the AOST need to be noted: (i) the NOST spans over one time step, and the AOST spans over two time steps; (ii) after the first time step, the solutions obtained by both the NOST and AOST are identical; (iii) solving the ADRE in two stages, the splitting introduces a time-lag between the ADE and RE. The time-lag breaks the actual physics of the ADRE and limits the applicability of the OST.

In the subsequent sections, analysis is discussed with respect to the time-lag error. The NOST is studied after every time step, and the AOST after every two time steps. Since analytical derivations can be made for the first time-step only, the analysis will first focus on the first time-step behavior followed by the long-term behavior

Advection–dispersion–reaction equation

Governing equation

The one-dimensional ADRE with first-order reaction under steady-state flow (i.e. constant volumetric moisture content and constant pore-water velocity) in a semi-infinite porous medium can be written in dimensionless form as

$$\frac{\partial C}{\partial T} = D^* \frac{\partial^2 C}{\partial X^2} - \frac{\partial C}{\partial X} - K^* C \qquad (1)$$

where $C = c/c_i$, $X = x/L$, $T = Vt/RL$, $D^* = D/VL$,

$K^* = KL/V$, c is the concentration of the contaminant, c_i is the influent concentration of the contaminant, x is the distance from the source, K is the first-order reaction rate, L is a characteristic length of the domain, t is the time, R is the retardation coefficient of the contaminant, V is the pore-water velocity, and D is the dispersion coefficient.[10]

Initial and boundary conditions

The ADRE given by eqn (1) is subjected to zero initial concentration over the domain. At the source, eqn (1) is subjected to the following Type-I or -III boundary condition given as

$$C(0,T) = \exp(-\lambda^* T) \tag{2a}$$

$$\left(-D^* \frac{\partial C}{\partial X} + C\right)_{X=0} = \exp(-\lambda^* T) \tag{2b}$$

In eqn (2a) or (2b), λ^* is an exponential term where $\lambda^* = 0$ and $\lambda^* \to \infty$ correspond to continuous and pulse boundary conditions, respectively. At the exit, eqn (1) is subjected to the following zero-dispersive boundary condition

$$\frac{\partial C}{\partial X}(\infty, T) = 0 \tag{3}$$

Analytical solutions

Type-I condition

Solution to eqn (1) subjected to boundary conditions given by eqns (2a) and (3) with zero initial concentration is obtained from Van Genuchten[15] as

$$C(X,T,K^*) = \exp(-\lambda^* T) P(X,T,K^*) \tag{4}$$

$$P(X,T,K^*) = \frac{1}{2}\exp\left\{\frac{(1-W)X}{2D^*}\right\} \operatorname{erfc}\left\{\frac{X - WT}{2(D^*T)^{1/2}}\right\} + \frac{1}{2}\exp\left\{\frac{(1+W)X}{2D^*}\right\} \operatorname{erfc}\left\{\frac{X + WT}{2(DT)^{1/2}}\right\} \tag{5a}$$

$$W(K^*) = \sqrt{1 + 4D^*(K^* - \lambda^*)} \tag{5b}$$

Type-III condition

Solution to eqn (1) subjected to boundary conditions given by eqns (2b) and (3) with zero initial condition is obtained from Van Genuchten[15] as

$$\begin{aligned} C(X,T,K^*) &= \exp(-\lambda^* T) F_1(X,T,K^*) \\ &\quad + F_2(X,T,K^*) \qquad \lambda^* \neq K^* \\ &= G(X,T,K^*) \qquad \lambda^* = K^* \end{aligned} \tag{6}$$

where

$$F_1(X,T,K^*) = F_3(-W,X,T,K^*) + F_3(W,X,T,K^*) \tag{7a}$$

$$F_2(X,T,K^*) = \frac{1}{2D^*(K^* - \lambda^*)} \exp\left\{\frac{X}{D^*} - K^* T\right\} \times \operatorname{erfc}\left\{\frac{X+T}{2(D^*T)^{1/2}}\right\} \tag{7b}$$

$$F_3(W,X,T,K^*) = \frac{1}{1-W} \exp\left\{\frac{(1+W)X}{2D^*}\right\} \times \operatorname{erfc}\left\{\frac{X+WT}{2(D^*T)^{1/2}}\right\} \tag{7c}$$

$$G(X,T,K^*) = \exp(-K^* T)[G_1(X,T) - G_2(X,T)] \tag{7d}$$

$$G_1(X,T) = \frac{1}{2}\operatorname{erfc}\left\{\frac{X-T}{2(D^*T)^{1/2}}\right\} + \left(\frac{T}{\Pi D^*}\right)^{1/2} \exp\left\{-\frac{(X-T)^2}{4D^*T}\right\} \tag{7e}$$

$$G_2(X,T) = \frac{1}{2}\left(1 + \frac{X}{D^*} + \frac{T}{D^*}\right) \times \exp\left\{\frac{X}{D^*}\right\} \operatorname{erfc}\left\{\frac{X+T}{2(D^*T)^{1/2}}\right\} \tag{7f}$$

Operator-splitting solutions after the first time step

Type-I condition

The OST splits the ADRE, eqn (1), into a corresponding ADE and a RE, and are given as

$$\frac{\partial C}{\partial T} = D^* \frac{\partial^2 C}{\partial X^2} - \frac{\partial C}{\partial X} \tag{8a}$$

$$\frac{dC}{dT} = -K^* C \tag{8b}$$

First, the ADE describing transport is solved over the time interval, $0 \leqslant T \leqslant \Delta T$, subjected to boundary conditions given by eqns (2a) and (3) with zero initial condition. This generates a nonreactive solution, $C_{NR}(X, \Delta T)$, obtained by substituting $T = \Delta T$ and $K^* = 0$ in eqn (4) as

$$C_{NR}(X,\Delta T) = \exp(-\lambda^* \Delta T) P(X,\Delta T, K^* = 0) \tag{9}$$

Finally, the RE describing reaction (decay) is integrated over $0 \leqslant T \leqslant \Delta T$ with $C_{NR}(X,\Delta T)$ as the initial condition to generate the operator-splitting solution, $C_{OS}(X,\Delta T)$, as

$$C_{OS}(X,\Delta T) = \exp(-K^* \Delta T - \lambda^* \Delta T) \times P(X,\Delta T, K^* = 0) \tag{10}$$

Type III condition
First, the ADE is solved subject to boundary conditions given by eqns (2b) and (3) with zero initial condition to generate

$$\begin{aligned} C_{NR}(X,\Delta T) &= \exp(-\lambda^*\Delta T)F_1(X,\Delta T,K^*=0) \\ &\quad + F_2(X,\Delta T,K^*=0) \qquad \lambda^* \neq 0 \\ &= G(X,\Delta T,K^*=0) \qquad \lambda^*=0 \end{aligned} \tag{11}$$

Finally, the RE is integrated to generate

$$\begin{aligned} C_{OS}(X,\Delta T) &= \exp(-K^*\Delta T - \lambda^*\Delta T) \\ &\quad \times F_1(X,\Delta T,K^*=0) \\ &\quad + F_2(X,\Delta T,K^*=0) \quad \lambda^* \neq 0 \\ &= \exp(-K^*\Delta T)G(X,\Delta T,K^*=0) \\ &\quad \lambda^*=0 \end{aligned} \tag{12}$$

It should be noted that eqns (10) and (12) are the operator-splitting solutions after the first time step for both NOST and AOST. Being derived analytically, these solutions are free of discretization errors. Hence, the discrepancy between these solutions from the corresponding exact analytical solutions should provide the inherent error caused by the time-lag of the OST.

Operator-splitting solutions after the *N*th time step

Normal operator-splitting
The NOST solution to the ADRE at the end of the Nth time step, $T_N = N\Delta T$, is obtained by computing between $T_{N-1} \leqslant T \leqslant T_N$. Since an analytical solution to the ADE with nonuniform initial conditions does not exist, NOST solution for $N > 1$ is obtained numerically. In order to obtain an analytical NOST solution free of discretization errors, each stage of the ADRE is solved by the finite difference method using a small space–time discretization. The actual time step, ΔT, is subdivided into M smaller time steps, ΔT_S (i.e. $\Delta T_S = \Delta T/M$; $M > 1$), and then the NOST solution at T_{N-1} is transported continuously over the interval $T_{N-1} \leqslant T \leqslant T_N$ across the M smaller ΔT_S. Finally, the solution thus obtained is decayed over ΔT across the M smaller ΔT_S to generate the analytical NOST solution at T_N.

Alternate operator-splitting
The AOST solution to the ADRE is studied over every two time steps. Thus, the AOST solution at T_N is obtained by computing between $T_{N-2} \leqslant T \leqslant T_N$. For reasons similar to the NOST, an analytical AOST solution is obtained numerically using the finite difference method with a small space–time discretization.

CRITERIA FOR THE CRITICAL ASSESSMENT

Mass balance error

The mass balance error (MBE) is defined as

$$E(N\Delta T) = 1 - \frac{M_{OS}(N\Delta T)}{M_{EX}(N\Delta T)} \tag{13}$$

where

$$M_{EX}(N\Delta T) = \int_0^\infty C(X,N\Delta T)\,dX \tag{14a}$$

$$M_{OS}(N\Delta T) = \int_0^\infty C_{OS}(X,N\Delta T)\,dX \tag{14b}$$

Here M_{EX} and M_{OS} are the total mass of contaminant in the system from the exact and OST solutions, respectively. If the OST solution decays more mass than the exact solution, then $M_{OS} < M_{EX}$ implying $E > 0$.

Concentration prediction error

The dimensionless concentration prediction error is defined as

$$S(X,N\Delta T) = C(X,N\Delta T) - C_{OS}(X,N\Delta T) \tag{15}$$

where C is the exact dimensionless concentration. If the OST solution generates a more decayed concentration than the exact solution, $C_{OS} < C$ implying $S > 0$. Moreover, from the definition of the dimensionless concentrations C and C_{OS}, it is noted that S represents the deviation of the OST concentration, c_{OS}, from the exact solution, c, as a fraction of the influent concentration, c_i.

Parameter sensitivity

The parameter sensitivity is defined as the partial derivative of the concentration prediction error, $S(X,T)$, with respect to a parameter of interest. Thus, the sensitivity determines the change in the difference between the exact and operator-splitting solution with respect to a unit change of the parameter. The concentration depends on ΔT, $D^*\Delta T$, $K^*\Delta T$ and $\lambda^*\Delta T$. However, it is observed that the mass balance error, concentration prediction error and sensitivity are basically dependent on $K^*\Delta T$ and $\lambda^*\Delta T$, and very little on ΔT and $D^*\Delta T$.[10] Hence in this study, the effects of $K^*\Delta T$ and $\lambda^*\Delta T$ only on the OST are addressed.

RESULTS AND DISCUSSION

The applicability of the OST is studied using a base problem. The applicability is assessed using the three different criteria: mass balance error, concentration prediction error and sensitivity. As the algorithm for the NOST spans over ΔT and that for the AOST over $2\Delta T$, the behavior of the NOST is studied after every

time step and that of the AOST over every two time steps. However, it should be noted that the algorithms of the NOST and the AOST over the first time step are identical, and hence, the result of the OST after the first time step is general for both NOST and AOST.

Base problem

The base problem is designed considering the facts that: (i) advection dominated problems are the most difficult to solve, and (ii) the OST is most sensitive to continuous boundary condition and $K^*\Delta T$.[13] The present analysis considers a base problem which is advection dominated and subjected to continuous boundary condition. The parameters thus assigned to the problem are: $\Delta T = 1$, $D^*\Delta T = 0{\cdot}2$, $K^*\Delta T = 0{\cdot}1$ and $\lambda^*\Delta T = 0$ with $K^*\Delta T$ and $\lambda^*\Delta T$ varied with different simulations.

Mass balance error

Type-III condition

Valocchi and Malmstead[13] considered the continuous boundary condition and derived analytically the mass balance errors after the first time step for both NOST and AOST. The present analysis extends their approach to derive the mass balance errors under a more general boundary condition given by eqn (2b). The details of the MBE derivations are given in Appendix A.

For the NOST, eqn (A10) of Appendix A gives the mass balance error when $\lambda^* \neq 0$ as

$$E(N\Delta T) = 1 - a\left(\frac{1-b}{a-b}\right)\left(1 - \frac{\ln a}{\ln b}\right) \quad \lambda^* \neq K^*$$

$$= 1 + \frac{1-a}{\ln a} \quad \lambda^* = K^* \quad (16)$$

where $a = \exp(-K^*\Delta T)$, $b = \exp(-\lambda^*\Delta T)$, and $N = [1, 2, 3, \ldots]$.

Similarly, for the AOST, eqn (A19) of Appendix A gives the mass balance error when $\lambda^* \neq 0$ as

$$E(N\Delta T) = 1 - (1-b)\left(1 - \frac{\ln a}{\ln b}\right)\left(\frac{a^2+b}{a^2-b^2}\right) \lambda^* \neq K^*$$

$$= 1 + \left(\frac{1}{2\ln a}\right)\left(a - \frac{1}{a}\right) \quad \lambda^* = K^* \quad (17)$$

where $N = [2, 4, 6, \ldots]$. Equations (16) and (17) show that the mass balance error of both NOST and AOST remain constant over time and depend on $K^*\Delta T$ and $\lambda^*\Delta T$. It should be noted that the mass balance error of the NOST remains constant after every time step while that of AOST remains constant after every two time steps.

For the continuous boundary condition ($\lambda^* = 0$), eqns (A12) and (A20) of Appendix A gives the mass balance error as

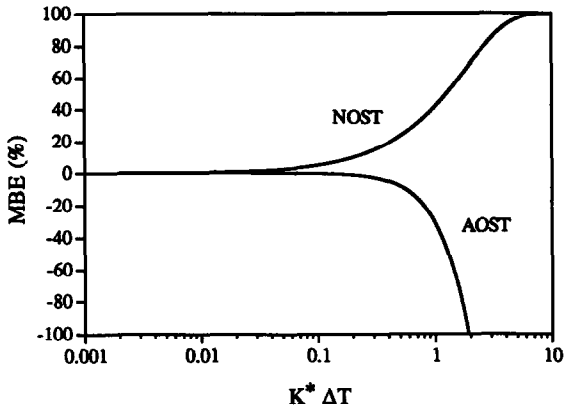

Fig. 1. Effect of $K^*\Delta T$ on the mass balance error (MBE) for Type-III boundary condition and $\lambda^* = 0$.

$$E(N\Delta T) = 1 - \frac{a}{a-1}\ln a \quad \text{for NOST}$$

$$= 1 - \frac{a^2+1}{a^2-1}\ln a \quad \text{for AOST} \quad (18)$$

where $N = [1, 2, 3, \ldots]$ for NOST and $N = [2, 4, 6, \ldots]$ for AOST. Figure 1 shows the results from eqn (18). The MBE increases as $K^*\Delta T$ increases. For $E = 5\%$, $K^*\Delta T \approx 0{\cdot}1$ for NOST and $K^*\Delta T \approx 0{\cdot}4$ for AOST, it is noted that the error for NOST is positive while that for AOST is negative. The positive error implies that the operator-splitting solution had decayed more mass than the exact solution. Under the exact solution, the mass input at the source over the time interval ΔT undergoes simultaneous transport and decay, and therefore, the mass input near the beginning of the interval undergoes longer decay than that input towards the end of the interval. Thus, the total mass input over an interval does not decay over the entire interval. On the contrary, with NOST, the total mass input during an interval decays over the entire interval, and the technique overestimates the amount of mass decayed. However the AOST shows a negative mass balance error. The negative error implies that the operator-splitting solution has decayed less mass than the exact solution. In the first time step, the AOST is identical to NOST and decays more mass than the exact solution. However, in the second time step, the reaction stage occurs before the transport stage allowing the AOST to decay less mass than the exact solution. Counteracting the mass balance errors in the two time steps, the AOST reduces the error in estimating the amount of mass decayed after two time steps.

Figure 2 shows the results from eqns (16) and (17) for $K^*\Delta T = 0{\cdot}1$. For the NOST, the mass balance error decreases as $\lambda^*\Delta T$ increases. However, for the AOST, the mass balance error decreases negatively as $\lambda^*\Delta T$ increases to a critical value at which the error becomes zero. As $\lambda^*\Delta T$ increases further, the error becomes positive, attains a maximum value and finally emerges with the tail of the NOST curve. Thus, the mass balance

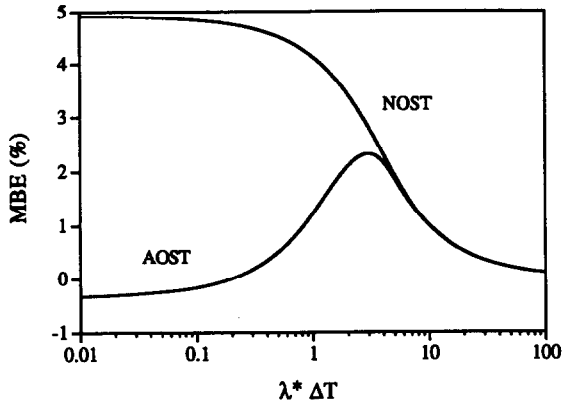

Fig. 2. Effect of $\lambda^*\Delta T$ on the mass balance error (MBE) for Type-III boundary condition and $K^*\Delta T = 0{\cdot}1$.

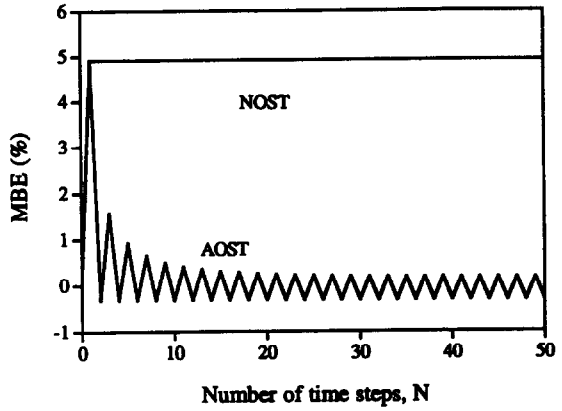

Fig. 3. Propagation of the mass balance error (MBE) for Type-III boundary condition with $\lambda^* = 0$ and $K^*\Delta T = 0{\cdot}1$.

error for both NOST and AOST is zero for pulse type boundary condition ($\lambda \to \infty$) as suggested by Valocchi and Malmstead.[13] At a large $\lambda^*\Delta T$, the input is rather instantaneous; most of the mass is provided at the beginning of the interval allowing a larger portion of the mass to undergo decay over the entire interval. This is a condition assumed by the NOST enabling it to approach the exact solution. In contrast, the scenario set by the AOST is rather complex. The AOST is counterbalancing the mass balance errors between two time steps which is a complex process of $\lambda^*\Delta T$ controlling the mass inflow. However, at large $\lambda^*\Delta T$, most of the mass is provided in the first time step allowing the AOST algorithm to approach the NOST algorithm, and the mass balance error becomes zero.

At this stage, it may be interesting to note the mass balance error for the AOST after odd time steps. Equation (A25) of Appendix A gives the mass balance error for the exponential boundary condition given by eqn (2b). However, only the error due to the continuous boundary condition is discussed here. From eqn (A26) of Appendix A, the error for the continuous boundary condition ($\lambda^* = 0$) is given as

$$E(N\Delta T) = 1 - \left(\frac{a \ln a}{a^N - 1}\right)\left(a^{N-1} + 2\frac{a^{N-1} - 1}{a^2 - 1}\right) \quad [N = 1, 3, 5, \ldots] \tag{19}$$

Equation (19) shows that the error varies over odd time steps. To study the propagation of the mass balance error over time, eqn (18) and eqn (19) are plotted for $K^*\Delta T = 0{\cdot}1$ over the first 20 time steps in Fig. 3. As per eqn (18), the figure shows a constant mass balance error after the first time step for NOST and after every two time steps for AOST. However, as per eqn (19), Fig. 3 shows that the mass balance errors for the AOST at odd time steps are positive and decays rapidly over time. Also the MBE approaches a constant value and the error is maximum at the first time step. As $K^*\Delta T > 0$, and $a < 1$, eqn (19) gives

$$\lim_{N \to \infty} E(N\Delta T) = 1 - \frac{2a}{a^2 - 1} \ln a \tag{20}$$

Thus, after sufficient time steps, the mass balance error does become constant. For the present problem, eqn (20) estimates the constant error to be $E(N \to \infty) = 0{\cdot}17\%$.

Type-I condition

From eqn (B6) of Appendix B, the mass balance error after the first time step is

$$E(\Delta T) = 1 - a\left[\frac{J(-\hat{W}, 0) + J(\hat{W}, 0)}{J(-W, K^*) + J(W, K^*)}\right] \tag{21}$$

where

$$J(W, K^*) = \frac{2D^*}{1 + W}\left[\frac{a}{b}\operatorname{erfc}\left(-\frac{1}{2}\sqrt{\frac{\Delta T}{D^*}}\right) - \operatorname{erfc}\left(-\frac{W}{2}\sqrt{\frac{\Delta T}{D^*}}\right)\right] \tag{22a}$$

$$\hat{W} = W(0) = \sqrt{1 - 4D^*\lambda^*} \tag{22b}$$

The mass balance error depends on ΔT, $D^*\Delta T$, $K^*\Delta T$ and $\lambda^*\Delta T$. However, for the base problem, Morshed[10] found that the error depends basically on $K^*\Delta T$ and $\lambda^*\Delta T$, and very little on ΔT and $D^*\Delta T$, much like the Type-III conditions. As the results for both Type-I and Type-III conditions are almost similar, Type I results are not shown here. The similarity in results may be due to the fact that the base problem is advection dominated converging the Type-I condition to the Type-III condition.

Concentration prediction error

Type-I condition

After the first time step. Morshed[10] derived the analytical solution to the concentration prediction

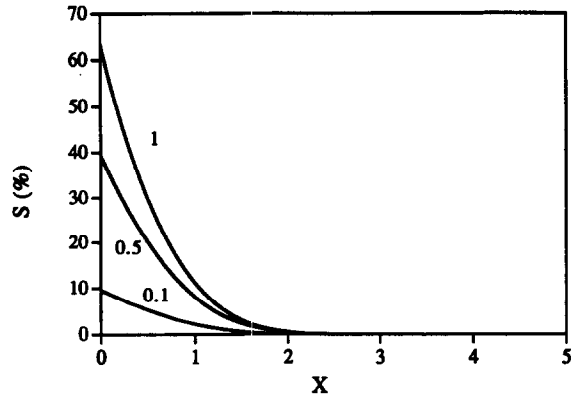

Fig. 4. Effect of $K^*\Delta T$ on concentration prediction error (S) for Type-I boundary condition with $\lambda^* = 0$, $D^*\Delta T = 0{\cdot}2$ and $\Delta T = 1$.

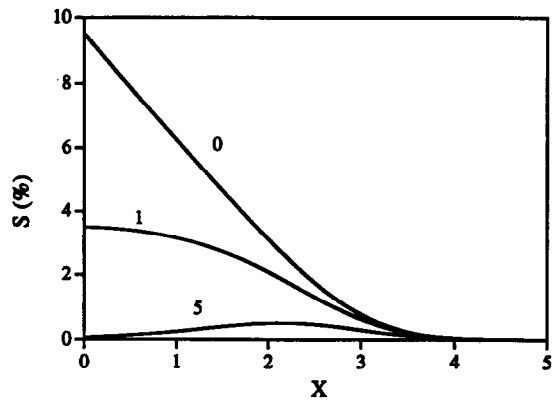

Fig. 5. Effect of $\lambda^*\Delta T$ on the concentration prediction error (S) for Type-I boundary condition with $K^*\Delta T = 0{\cdot}1$, $D^*\Delta T = 0{\cdot}2$ and $\Delta T = 1$.

error after the first time step incurred by the OST. Here, the analytical derivations are not provided for space limitations, and only the results are presented. For the base problem, Fig. 4 shows the effect of varying $K^*\Delta T$ on the error after the first time step. The error decays rapidly over distance, being maximum at the source. As $K^*\Delta T$ increases, the error curves move upward depicting an increase in the error. However, all the curves intersect at zero error indicating that the distance beyond which the error becomes negligible is independent of $K^*\Delta T$. For $K^*\Delta T = 0{\cdot}1$, Fig. 4 shows the concentration prediction error at the source to be 10% while Fig. 1 shows the overall mass balance error to be 5%.

For the base problem, Fig. 5 shows the effect of varying $\lambda^*\Delta T$ on the concentration prediction error after the first time step. As $\lambda^*\Delta T$ increases, the error curves move downward depicting a decrease in error and shifts the maximum error location away from the source showing the control of λ^* on mass inflow. For a continuous boundary condition ($\lambda^* = 0$), the error decays over distance with a maximum at the source. For a pulse boundary condition ($\lambda^* \to \infty$), the error is zero and the OST generates the exact solution. Also, all the curves intersect at zero error indicating that the distance beyond which the error becomes negligible is independent of $\lambda^*\Delta T$.

Figures 4 and 5 show that the OST solutions are most affected near the source boundary. Over the first time step, the OST performs first the transport stage maintaining exact boundary conditions. However, decaying this transport solution in the next stage, the OST affects the actual boundary condition. Hence, the solution is affected near the boundaries where the concentration is the highest. Figures 4 and 5 also suggest that the concentration prediction error of a given problem is larger than its overall mass balance error. Thus, in applying the OST, a $K^*\Delta T$ much smaller than that obtained using a mass balance error criterion should be used for an accurate solution.

Propagation over time. The base problem is solved numerically over the first 20 time steps using the NOST. As the problem is solved with $K^*\Delta T = 0{\cdot}1$, the mass balance error is expected to be 5% (Fig. 1). In order to study the AOST solutions under the same mass balance error, the base problem is solved over the same time period using AOST but with a revised $K^*\Delta T = 0{\cdot}4$ (Fig. 1). Small space–time discretization is used to obtain the analytical OST solutions. Figure 6 shows the concentration prediction error for the NOST. The error is positive showing that the OST concentration is less than the exact concentration. Also, the error near the source remains constant over time, and a short distance away from the source, the error dampens and spreads. Figure 7 shows the concentration prediction errors for AOST. At even time steps ($N = 10$ and 20), the error is zero at the source, increases to a negative maximum some distance away from the source, and finally decays back to zero further away from the source. The zero error at the source is due to the fact that the transport stage is solved after the reaction stage at even time steps allowing the OST to maintain an exact boundary condition. The negative error after the source shows that the OST concentration is greater than the exact concentration. At odd time steps ($N = 5$ and 15), the error is maximum at the source and decreases rapidly with distance away from the source. The error is positive showing that the OST concentration is smaller than the exact concentration. It is noted that the concentration prediction error at the source remains constant at 32% while the mass balance error varies from 19% after the first time step (eqn (19)) to 0·03% after many time steps (eqn (20)). Moreover, the error at even time steps is much smaller than at odd time steps. Thus, the AOST solutions at even time steps should only be taken into account, and the odd time step solutions should be discarded. It is further noted that the errors at even and odd time steps remain constant and follow two distinctly different trajectories. The oscillation of the error between negative and positive values signifies the

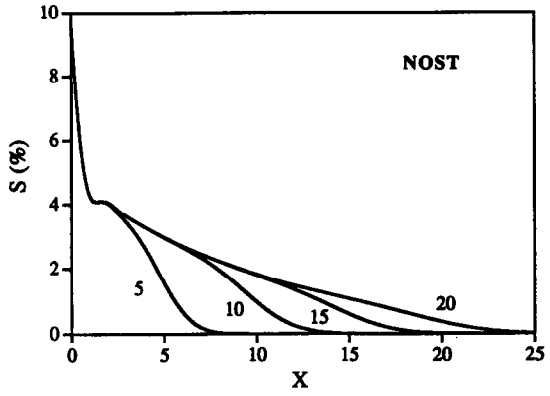

Fig. 6. Propagation of the concentration prediction error (S) of NOST for Type-I boundary condition with $\lambda^* = 0$, $K^*\Delta T = 0{\cdot}1$, $D^*\Delta T = 0{\cdot}2$ and $\Delta T = 1$.

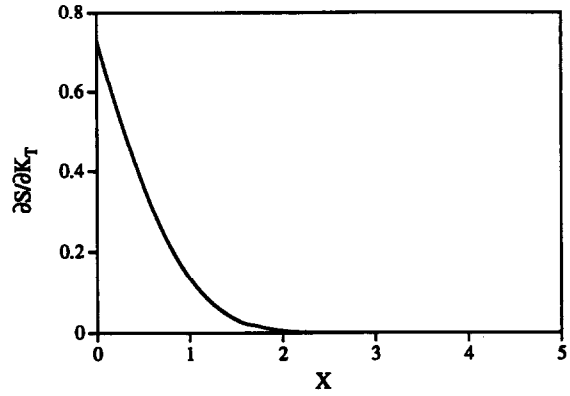

Fig. 8. Sensitivity of the concentration prediction error to $K_T = K^*\Delta T, \partial S/\partial K_T$, for Type-III boundary condition with $\lambda^* = 0$, $K^*\Delta T = 0{\cdot}1$, $D^*\Delta T = 0{\cdot}2$ and $\Delta T = 1$.

counterbalancing effect of the AOST over every two time steps. This counterbalancing procedure basically allows the AOST to generate a solution superior to that of the NOST. Both the NOST (Fig. 6) and the AOST (even time steps, Fig. 7) results show a maximum deviation of 10%. However, the AOST solution is obtained using a time-lag four times greater than that used to obtain the NOST solution.

Type-III condition

Morshed[10] derived the analytical solution to the concentration prediction error after the first time step incurred by the OST. In addition, the propagation of the error over a given simulation period for both NOST and AOST was studied. The results showed that the Type-III solutions are similar to the Type-I solutions and are therefore not shown here.

Parameter sensitivity

Type-III condition

Morshed (1994) derived the analytical solution for the sensitivity of the OST solution after the first time step to different parameters. For the base problem, Fig. 8 shows the sensitivity of the concentration prediction error to $K_T = K^*\Delta T$. The sensitivity is maximum at the source and decreases gradually over distance from the source. Thus, an increase in $K^*\Delta T$ increases the concentration prediction error with a maximum at the source. For the same problem, Fig. 9 shows the sensitivity of the concentration prediction error to $\lambda_T = \lambda^*\Delta T$. The sensitivity is negative, and it is maximum at the source and decreases gradually over distance from the source. The negative sensitivity implies that the concentration prediction error decreases as $\lambda^*\Delta T$ increases. The results of the sensitivity analysis agrees with earlier observations where the OST solution deteriorates as $K^*\Delta T$ increases and improves as $\lambda^*\Delta T$ increases.

Type-I condition

Morshed[10] derived the analytical solution for the sensitivity of the OST solution after the first time step to different parameters. The results showed that Type-I solutions are similar to Type-III solutions and are therefore not shown here. However, the Type-I sensitivities are found to be slightly higher than the corresponding Type-III sensitivities. The exact concentration at the source for the Type-I is equal to the influent concentrations

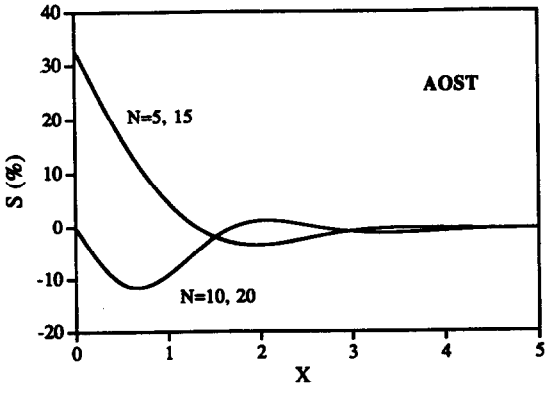

Fig. 7. Propagation of the concentration prediction error (S) of AOST for Type-I boundary condition with $\lambda^* = 0$, $K^*\Delta T = 0.4$, $D^*\Delta T = 0{\cdot}2$ and $\Delta T = 1$.

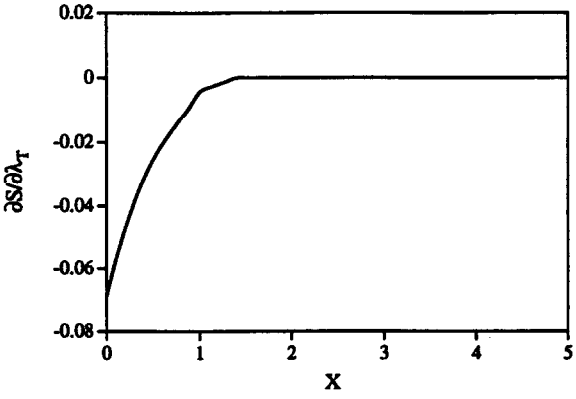

Fig. 9. Sensitivity of the concentration prediction error to $\lambda_T = \lambda^*\Delta T, \partial S/\partial \lambda_T$, for Type-III boundary condition with $\lambda^* = 0$, $K^*\Delta T = 0{\cdot}1$, $D^*\Delta T = 0{\cdot}2$ and $\Delta T = 1$.

while that for the Type-III is less than the influent concentration. As per eqn (8b), the reaction stage of the OST is independent of boundary condition and proportional to concentration. Therefore the OST decays more mass for a Type-I condition than for a Type-III. Therefore it appears that the OST is more sensitive to Type-I conditions than to Type-III conditions.

SUMMARY AND CONCLUSIONS

The study was performed to assess the accuracy of the operator-splitting technique in solving the advection–dispersion–reaction problems. The study considered two variations of the technique namely, the normal operator-splitting technique and the alternate operator-splitting technique. The one-dimensional advection–dispersion–reaction equation with first-order reaction was solved using each of these techniques, and the effects of splitting on the accuracy of each technique was evaluated and compared. Also, estimates of the mass balance error incurred by each technique were made for efficient implementation of the operator-splitting technique.

The following specific conclusions can be made from the study.

1. The splitting of the advection–dispersion–reaction equation introduces an inherent error in the operator-splitting technique. This inherent error is referred to here as the time-lag error.
2. The time-lag error directly depends on the reaction rate and the time-lag itself. Therefore, an advection–dispersion–reaction equation involving fast reaction should be split with a small time-lag.
3. The time-lag to be used in the splitting should not be solely based on the mass balance error criterion.
4. The operator-splitting technique is most sensitive to the continuous boundary condition and least to the pulse boundary condition. The technique generates the exact solution for the pulse condition.
5. The operator-splitting technique is most sensitive to a Type-I boundary condition than to a Type-III boundary condition.
6. The alternate operator-splitting technique is superior to the normal operator-splitting technique provided the alternate operator-splitting solution at even time steps is only considered.
7. The maximum error occurs near the source for the normal operator-splitting solution and some distance downstream from the source for the alternate operator-splitting solution.
8. The mass balance error remains constant after every time step for the normal operator-splitting technique and after every two time steps for the alternate operator-splitting technique.
9. The error in the normal operator-splitting solution spreads over time. In contrast, the errors in the alternate operator-splitting solution oscillates over time between two constant trajectories, one for the even time steps and the other for the odd time steps.

ACKNOWLEDGMENT

The financial support for this research was provided through the Utah Water Research Laboratory, Utah State University, Logan, Utah.

REFERENCES

1. Borden, R. C. & Bedient, P. B. Transport of dissolved hydrocarbons influenced by oxygen-limited biodegradation: 1. Theoretical development. *Water Resour. Res.*, **22**(13) (1986) 1973–82.
2. Celia, M. A., Kindred, J. S. & Hererra, I. Contaminant transport and biodegradation: 1. A numerical model for reactive transport in porous media. *Water Resour. Res.*, **25**(6) (1989) 1141–48.
3. Chiang, C. Y., Dawson, C. N. & Wheeler, M. F. Modeling of In-situ Biorestoration of Organic Compounds in Groundwater. Research Report UH/MD-68, Department of Mathematics, University of Houston, Houston, Texas, 1991.
4. Chiang, C. Y., Wheeler, M. F. & Bedient, P. B. A modified method of characteristics technique and mixed finite elements method for simulation of groundwater solute transport. *Water Resour. Res.*, **25**(7) (1989) 1541–9.
5. Douglas, J. Jr & Russell, T. F. Numerical methods for convection-dominated diffusion problems based on combining the methods of characteristics with finite element or finite difference procedures. *SIAM J. Num. Anal.*, **19**(5) (1982) 871–85.
6. Kindred, J. S. & Celia, M. A. Contaminant transport and biodegration: 2. Conceptual model and test simulations. *Water Resour. Res.*, **25**(6) (1989) 1149–59.
7. Kinzelbach, W., Schäefer, W. & Herzer, J. Numerical modeling of natural and enhanced denitrification processes in aquifers. *Water Resour. Res.*, **27**(6) (1991) 1123–35.
8. LeVeque, R. & Oliger, J. Numerical methods based on additive splittings for hyperbolic partial differential equations. *Math. Comp.*, **40**(162) (1983) 469–97.
9. Miller, C. T. & Rabideau, A. J. Development of split-operator, Petrov–Galerkin methods to simulate transport and diffusion problems. *Water Resour. Res.*, **29**(7) (1993) 2227–40.
10. Morshed, J. Critical Assessment of the Operator-Splitting Technique in Solving the Advection–Dispersion–Reaction Problems. MS Thesis, Utah State University, Logan, Utah, 1994.
11. Rifai, H. S. & Bedient, P. B. Comparison of biodegradation kinetics with an instantaneous reaction model for groundwater. *Water Resour. Res.*, **26**(4) (1990) 637–45.
12. Strang, G. On the construction and comparison of difference schemes. *SIAM J. Num. Anal.*, **5**(3) (1968) 506–17.
13. Valocchi, A. J. & Malmstead, M. Accuracy of the operator splitting for advection–dispersion–reaction problems. *Water Resour. Res.*, **28**(5) (1992) 1471–6.

14. Valocchi, A. J., Odencrantz, J. E. & Rittmann, B. E. Computational studies of the transport of reactive solutes: Interaction between adsorption and biotransformation. In *Advances in Hydro-Science and Engineering, Proc. 1st Int. Conf. on Hydro-Science and Engineering*. Washington, D.C., Vol. I, Part B, 1993, pp. 1845–52.
15. Van Genuchten, M. T., Analytical solutions for chemical transport with simultaneous adsorption, zero-order production and first-order decay. *J. Hydrol.*, **49** (1981) 213–33.
16. Wheeler, M. F. Modeling of highly advective problems. In *Computational Methods in Water Resources. Vol. 1, Modeling Surface and Sub-Surface Flows*, ed. M. A. Celia, L. A. Ferrand, C. A. Brebbia, W. G. Gray & G. F. Pinder. Elsevier, Amsterdam, 1988, pp. 35–44.
17 Wheeler, M. F. & Dawson, C. N. An Operator-Splitting Method for Advection–Diffusion–Reaction Problems. Technical Report 87-9, Department of Mathematical Sciences, Rice University, Houston, Texas, 1987.
18. Wheeler, M. F., Dawson, C. N., Bedient, P. B., Chiang, C. Y., Borden, R. C. & Rifai, H. S. Numerical simulation of microbial biodegradation of hydrocarbons in groundwater. In *Proc. NWWA Conf. on Solving Groundwater Problems with Models*. National Water Well Association, Dublin, OH, USA, 1987, pp. 92–109.

APPENDIX A: MASS BALANCE ERROR FOR A TYPE-III BOUNDARY CONDITION

Exact mass

Integrating the ADRE, eqn (1), over the column length, we obtain

$$\frac{\mathrm{d}}{\mathrm{d}T}\int_0^\infty C(X,T)\,\mathrm{d}X + K^*\int_0^\infty C(X,T)\,\mathrm{d}X = \int_0^\infty \left[D^*\frac{\partial^2 C}{\partial X^2} - \frac{\partial C}{\partial X}\right]\mathrm{d}X \tag{A1}$$

and using eqn (14a)

$$\frac{\mathrm{d}M_{\mathrm{EX}}(T)}{\mathrm{d}T} + K^* M_{\mathrm{EX}}(T) = \left[D^*\frac{\partial C}{\partial X} - C\right]_0^\infty \tag{A2}$$

Applying the boundary conditions, eqns (2b) and (3), and the assumption $C(\infty, T) = 0$ to eqn (A2),

$$\frac{\mathrm{d}M_{\mathrm{EX}}(T)}{\mathrm{d}T} + K^* M_{\mathrm{EX}}(T) = \exp(-\lambda^* T) \tag{A3}$$

Integrating eqn (A3) using the zero initial condition, $M_{\mathrm{EX}}(0) = 0$, we obtain

$$M_{\mathrm{EX}}(N, \Delta T) = \frac{a^N - b^N}{\ln a - \ln b}\Delta T \qquad \lambda^* \neq K$$
$$= a^N N \Delta T \qquad \lambda^* = k^* \tag{A4}$$

where $T = N\Delta T$, $a = \exp(-K^*\Delta T)$ and $b = \exp(-\lambda^*\Delta T)$.

Mass balance errors

Normal operator-splitting

The ADRE is split as

$$\frac{\partial C_{\mathrm{NR}}}{\partial T} = D^*\frac{\partial^2 C_{\mathrm{NR}}}{\partial X^2} - \frac{\partial C_{\mathrm{NR}}}{\partial X} \tag{A5a}$$

$$\frac{\mathrm{d}C_{\mathrm{OS}}}{\mathrm{d}T} = -K^* C_{\mathrm{OS}} \tag{A5b}$$

Integrating eqn (A5a) and (A5b) over the entire column

$$\frac{\mathrm{d}M_{\mathrm{NR}}(T)}{\mathrm{d}T} = \exp(-\lambda^* T) \tag{A6a}$$

$$\frac{\mathrm{d}M_{\mathrm{OS}}(T)}{\mathrm{d}T} = -K^* M_{\mathrm{OS}}(T) \tag{A6b}$$

Integrating eqn (A6a) over the time interval, $T_{N-1} \leqslant T \leqslant T_N$, with $M_{\mathrm{NR}}(T_{N-1}) = M_{\mathrm{OS}}(T_{N-1})$, and integrating eqn (A6b) over the same time interval with $M_{\mathrm{OS}}(T_{N-1}) = M_{\mathrm{NR}(\mathrm{T_N})}$, the solution for $\lambda^* \neq 0$ is

$$M_{\mathrm{NR}}(T_N) = M_{\mathrm{OS}}(T_{N-1}) - \frac{(1-b)b^{N-1}}{\ln b}\Delta T \tag{A7a}$$

$$M_{\mathrm{OS}}(T_N) = aM_{\mathrm{NR}}(T_N) \tag{A7b}$$

Substituting eqn (A7a) in eqn (A7b)

$$M_{\mathrm{OS}}(T_N) = aM_{\mathrm{OS}}(T_{N-1}) - a\frac{(1-b)b^{N-1}}{\ln b}\Delta T$$
$$= aM_{\mathrm{OS}}(T_{N-1}) + Ab^{N-1} \tag{A8}$$

where

$$A = -a\frac{1-b}{\ln b}\Delta T = a\frac{1-b}{\ln(1/b)}\Delta T.$$

Now, considering zero initial mass, $M_0 = 0$

$$M_{\mathrm{OS}}(T_1) = aM_{\mathrm{OS}}(T_0) + Ab^0 = A$$
$$M_{\mathrm{OS}}(T_2) = aM_{\mathrm{OS}}(T_1) + Ab^1 = A(a+b)$$
$$M_{\mathrm{OS}}(T_3) = aM_{\mathrm{OS}}(T_2) + Ab^2 = A(a^2 + ab + b^2)$$
$$M_{\mathrm{OS}}(T_4) = aM_{\mathrm{OS}}(T_3) + Ab^3 = (A^3a^2b + ab^2 + b^3)$$
$$\vdots$$
$$M_{\mathrm{OS}}(T_N) = aM_{\mathrm{OS}}(T_{N-1}) + Ab^{N-1}$$
$$= A(a^{N-1} + a^{N-2}b + a^{N-3}b^2 + \cdots + b^{N-1})$$

Thus,

$$M_{\mathrm{OS}}(T_N) = Aa^{N-1}\left(1 + \frac{b}{a} + \left(\frac{b}{a}\right)^2 + \cdots + \left(\frac{b}{a}\right)^{N-1}\right)$$

implying

$$M_{\mathrm{OS}}(T_N) = \frac{a^N - b^N}{a-b}\frac{a(1-b)}{\ln(1/b)}\Delta T \qquad \lambda^* \neq K^*$$
$$= Na^N\frac{(1-b)}{\ln(1/b)}\Delta T \qquad \lambda^* = K^* \tag{A9}$$

From eqn (13), the mass balance error becomes

$$E(N\Delta T) = 1 - a\left(\frac{1-b}{a-b}\right)\left(1 - \frac{\ln a}{\ln b}\right) \qquad \lambda^* \neq K^*$$

$$= 1 + \frac{1-a}{\ln a} \qquad \lambda^* = K^* \text{(A10)}$$

For $\lambda^* = 0$, it is noted that $b = 1$ and

$$\underset{b\to 1}{\text{Limit}} \frac{1-b}{\ln b} = -1 \tag{A11}$$

Thus, applying eqn (A11) to eqn (A10),

$$E(N\Delta T) = 1 - \left(\frac{a}{a-1}\right)\ln a \tag{A12}$$

Alternate operator-splitting

Even time steps. A two-time step interval, $T_{N-2} \leqslant T \leqslant T_N$ where $N = [2,4,6,\ldots]$, is considered. In the first time step, the algorithm is identical to NOST, and for $\lambda^* \neq 0$, eqn (A8) gives

$$M_{OS}(T_{N-1}) = aM_{OS}(T_{N-2}) - a\frac{(1-b)b^{N-2}}{\ln b}\Delta T \tag{A13}$$

In next time step, the reaction equation is first solved. Thus, using eqn (A7b), the reactive mass at T_N becomes

$$M_R(T_N) = aM_{OS}(T_{N-1}) \tag{A14}$$

Finally, after transporting the reactive mass using eqn (A7a),

$$M_{OS}(T_N) = M_R(T_{N-1}) - \frac{(1-b)b^{N-1}}{\ln b}\Delta T \tag{A15}$$

Substituting eqn (A14) in eqn (A15),

$$M_{OS}(T_N) = aM_{OS}(T_{N-1}) - \frac{(1-b)b^{N-1}}{\ln b}\Delta T \tag{A16}$$

Substituting eqn (A13) in (A16),

$$M_{OS}(T_N) = a^2 M_{OS}(T_{N-2}) - (a^2+b)\frac{(1-b)b^{N-2}}{\ln b}\Delta T \tag{A17}$$

Equation (A17) is in recursive form for even time steps. Considering this recursive equation and zero initial, Morshed[10] deduced

$$M_{OS}(T_N) = (a^2+b)\left(\frac{1-b}{\ln(1/b)}\right)\left(\frac{a^N - b^N}{a^2-b^2}\right)\Delta T \qquad \lambda^* \neq K^*$$

$$= \frac{a^{N-1}(1-a^2)}{2\ln a} N\Delta T \qquad \lambda^* = K^* \tag{A18}$$

From eqn (13), the mass balance error becomes

$$E(N\Delta T) = 1 - (1-b)\left(1 - \frac{\ln a}{\ln b}\right)\left(\frac{a^2+b}{a^2-b^2}\right) \qquad \lambda^* \neq K^*$$

$$= 1 - \left(\frac{1}{2\ln a}\right)\left(a - \frac{1}{a}\right) \qquad \lambda^* = K^* \tag{A19}$$

For $\lambda^* = 0$, applying the limit given by eqn (A11) to eqn (A19),

$$E(N\Delta T) = 1 - \left(\frac{a^2+1}{a^2-1}\right)\ln a \tag{A20}$$

Odd time steps. In eqn (A13), it is noted that T_{N-1} and T_{N-2} are the odd and even time steps, respectively. Thus, $M_{OS}(T_{N-2})$ in eqn (A13) can be obtained from eqn (A16) using $N \leftarrow N-2$, and for $\lambda^* \neq 0$, this generates

$$M_{OS}(T_{N-2}) = aM_{OS}(T_{N-3}) - \frac{(1-b)b^{N-3}}{\ln b}\Delta T \tag{A21}$$

Substituting eqn (A21) in eqn (A13),

$$M_{OS}(T_{N-1}) = a^2 M_{OS}(T_{N-3}) - ab^{N-3}\left(\frac{1-b^2}{\ln b}\right)\Delta T \tag{A22}$$

Putting $N \leftarrow N+1$ in eqn (A22),

$$M_{OS}(T_N) = a^2 M_{OS}(T_{N-2}) - ab^{N-2}\left(\frac{1-b^2}{\ln b}\right)\Delta T \tag{A23}$$

where now $N = [1,3,5,\ldots]$. Equation (A23) is a recursive equation for odd time steps. For zero initial mass, Morshed[10] showed that

$$M_{OS}(T_N) = \frac{a(1-b)}{\ln(1/b)} \times \left[a^{N-1} + \frac{a^{N-1} - b^{N-1}}{a^2-b^2}(1+b)b\right]\Delta T \qquad \lambda^* \neq K^*$$

$$= a^{N-1}\left(\frac{a-1}{2\ln a}\right)[(a-1) + (a+1)N]\Delta T \qquad \lambda^* = K^* \tag{A24}$$

From eqn (13), the mass balance error becomes

$$E(N\Delta T) = 1 - a\left(1 - \frac{\ln a}{\ln b}\right)\left(\frac{1-b}{a^N - b^N}\right) \times \left[a^{N-1} + \frac{a^{N-1} - b^{N-1}}{a^2 - b^2}(1+b)b\right] \qquad \lambda^* \neq K^*$$

$$= 1 - \left(\frac{a-1}{2a\ln a}\right)\left[(a-1)\frac{1}{N} + (a+1)\right] \qquad \lambda^* = K^* \tag{A25}$$

For $\lambda^* = 0$, applying the limit given by eqn (A11) to eqn (A25),

$$E(N\Delta T) = 1 - \left(\frac{a}{a^N - 1}\right)\left(a^{N-1} + 2\frac{a^{N-1} - 1}{a^2 - 1}\right)\ln a \tag{A26}$$

APPENDIX B: MASS BALANCE ERROR FOR TYPE-I BOUNDARY CONDITION

Exact mass

Substituting eqn (4) in eqn (14a),

$$M_{EX}(\Delta T) = \tfrac{1}{2}b[J(-W, K^*) + J(W, K^*)] \tag{B1}$$

where

$$J(W, K^*) = \int_0^\infty \exp\left\{\frac{(1+W)X}{2D^*}\right\} \times \operatorname{erfc}\left\{\frac{X + W\Delta T}{2(D\Delta T)^{1/2}}\right\} dX \tag{B2}$$

Morshed[10] evaluated $J(W, K^*)$ and it is given by eqn (22).

Mass balance errors

Normal operator-splitting

In the first stage, the ADE is solved with $K^* = 0$. Hence, the non-reactive mass is obtained from eqn (B1) as

$$M_{NR}(\Delta T) = \tfrac{1}{2}b[J(-\hat{W}, 0) + J(\hat{W}, 0)] \tag{B3}$$

In the second stage, the non-reactive mass of the first stage is decayed. This requires the solution of eqn (A6b) given by eqn (A7b). Thus,

$$M_{OS}(\Delta T) = aM_{NR}(\Delta T) \tag{B4}$$

Substituting eqn (B3) in eqn (B4)

$$M_{OS}(\Delta T) = \tfrac{1}{2}ab[J(-\hat{W}, 0) + (\hat{W}, 0)] \tag{B5}$$

From eqn (13), the mass balance error becomes

$$E(\Delta T) = 1 - a\left[\frac{J(-\hat{W}, 0) + J(\hat{W}, 0)}{J(-W, K^*) + J(W, K^*)}\right] \tag{B6}$$